Determination of the Orientation of a Band 3 Affinity Spin-Label Relative to the Membrane Normal Axis of the Human Erythrocyte†

Eric J. Hustedt and Albert H. Beth*

Department of Molecular Physiology and Biophysics, Vanderbilt University, Nashville, Tennessee 37232-0615

Received January 22, 1996; Revised Manuscript Received March 25, 1996⊗

ABSTRACT: The orientation of the nitroxide moiety of an isotopically substituted spin-labeled derivative of dihydrostilbenedisulfonate ([^{15}N,^{2}H$_{13}$]-SL-H$_2$DADS-maleimide) covalently coupled at the extracellular stilbenedisulfonate binding site of the human erythrocyte anion exchange protein, band 3, has been determined relative to the membrane normal axis of intact cells. The X-band linear electron paramagnetic resonance (EPR) spectra of [^{15}N,^{2}H$_{13}$]-SL-H$_2$DADS-maleimide-labeled band 3 in intact erythrocytes oriented by flow through an EPR flat cell have been obtained for two orthogonal orientations of the sample in the DC magnetic field. Two different methods of analysis have provided very similar values for the angles α_1 and β_1 which uniquely define the orientation of the nitroxide axis frame relative to the membrane normal axis. In the first approach, a variable fraction of the cells, *f*, were taken to be biconcave disks perfectly oriented relative to the flat cell surface with the remainder, $1 - f$, isotropically oriented. Simultaneous nonlinear least squares analysis of the spectra obtained at the two sample orientations yielded best fit values of $f = 0.60$, $\alpha_1 = 58°$, and $\beta_1 = 36°$. In the second approach, the EPR spectra of flow-oriented intact erythrocytes labeled with the fatty acid spin-label, [^{15}N,^{2}H$_{12}$]-5-nitroxyl stearate, have been obtained at the two sample orientations. These two spectra have been used to determine a model-independent distribution of membrane normal orientations in the sample. Using this experimentally determined membrane normal orientation distribution, the EPR spectra of [^{15}N,^{2}H$_{13}$]-SL-H$_2$DADS-maleimide-labeled erythrocytes were then reanalyzed to obtain a second determination of the nitroxide orientation, $\alpha_1 = 61°$ and $\beta_1 = 37°$. The orientation of the nitroxide with respect to the membrane normal axis determined in the present study is nearly identical to the orientation of the nitroxide with respect to the uniaxial rotational diffusion axis, $\alpha = 66°$ and $\beta = 34°$, as determined from saturation transfer EPR (ST-EPR) studies [Hustedt, E. H., & Beth, A. H. (1995) *Biophys. J. 69*, 1409−1423]. This result supports the conclusion that the motion observed using ST-EPR spectroscopy is, in fact, the uniaxial rotational diffusion of band 3 about the membrane normal.

The characterization of the rotational dynamics of integral membrane proteins can provide important insights into the nature of various protein−protein and protein−lipid interactions within the lipid bilayer. The rotational dynamics of a membrane protein should be highly sensitive to the size of the integral membrane domain (Saffman & Delbrück, 1975) and hence to the oligomeric state(s) of the protein and to the mechanical rigidity of other specific protein−protein complexes involving cytoplasmic or cytostolic domains. As a result, numerous studies have been reported in the literature describing the use of exogenous molecular probes covalently coupled to membrane proteins as reporters of rotational dynamics [for reviews, see Cherry (1978, 1981), Garland and Johnson (1985), Thomas (1985, 1986), and Jovin and Vaz (1989)]. One of the integral membrane proteins most widely studied using this approach has been the anion exchange protein of the human erythrocyte membrane, known as band 3.

Early work by Cherry and co-workers (Cherry et al., 1976) showed that the long lifetime triplet probe, eosin, could be covalently coupled to band 3 and used to study the rotational dynamics of the protein in erythrocyte ghost membranes by measuring the transient absorption dichroism following polarized excitation of eosin to its triplet state. Subsequently, a number of laboratories have reported studies of the rotational dynamics of eosin-labeled band 3 using either transient dichroism or time-resolved phosphorescence emission anisotropy methods (Nigg & Cherry, 1979a,b, 1980; Austin et al., 1979; Mühlbach & Cherry, 1982, 1985; Tsuji et al., 1988; Matayoshi & Jovin, 1991; Tilley et al., 1991; McPherson et al., 1992, 1993; Corbett & Golan, 1993). Collectively, these studies have shown that the polarization anisotropy decay of eosin-labeled band 3 in ghost membranes is a complicated, multiexponential function with decay rates ranging from approximately 10 μs to approximately 10 ms (Matayoshi & Jovin, 1991).

Saturation transfer electron paramagnetic resonance (ST-EPR) offers an alternative experimental method for the study of the rotational dynamics of membrane proteins (Thomas, 1985, 1986; Beth & Robinson, 1989). Recently, nitroxide spin-labels which affinity label band 3 in intact erythrocytes have been reported and used to study the rotational diffusion of band 3 using ST-EPR (Beth et al., 1986; Anjaneyulu et al., 1988, 1989). Most recently, an isotopically substituted spin-labeled derivative of dihydrostilbenedisulfonate ([^{15}N,^{2}H$_{13}$]-SL-H$_2$DADS-maleimide) has been reported (Wojcicki & Beth, 1993).

† This work was supported by grants from the National Institutes of Health (HL34737 and RR04075). E.J.H. was supported by NIH Training Grant T32 DK07186.

* Address correspondence to Dr. Albert H. Beth, Department of Molecular Physiology and Biophysics, 727 Light Hall, Vanderbilt University, Nashville, TN 37232-0615.

⊗ Abstract published in *Advance ACS Abstracts,* May 1, 1996.

S0006-2960(96)00151-1 CCC: $12.00

Scothorn et al. (1996) have shown that, under the conditions employed in this work, [^{15}N,^{2}H$_{13}$]-SL-H$_2$DADS-maleimide reacts specifically with band 3 in intact erythrocytes. At the labeling concentration employed, approximately 1 mol of the label is covalently bound per mole of band 3 monomer and band 3-mediated anion exchange is completely inhibited. The labeling of band 3 with [^{15}N,^{2}H$_{13}$]-SL-H$_2$DADS-maleimide is blocked by prelabeling erythrocytes with 4,4′-diisothiocyanostilbene-2,2′-disulfonate (DIDS) or eosin-5-maleimide, and the covalent reaction site for the probe is on the same 17K fragment which is labeled by eosin-5-maleimide (Cobb & Beth, 1990) and H$_2$DIDS (Okubo et al., 1994). These observations all support the conclusion that [^{15}N,^{2}H$_{13}$]-SL-H$_2$DADS-maleimide is reacting at the extracellular stilbenedisulfonate binding site on band 3 and further suggest a unique reaction site.

The global rotational dynamics of a large integral membrane protein such as band 3 are expected to be dominated by the rotational diffusion of the integral membrane domain about the membrane normal axis (Saffman & Delbrück, 1975). For both time-resolved absorption (Cherry & Godfrey, 1981) or emission (Garland & Johnson, 1985) anisotropy studies using triplet probes and ST-EPR (Beth et al., 1983; Beth & Robinson, 1989) studies using spin-label probes, the experimental results for a protein undergoing uniaxial rotational diffusion are determined by both the uniaxial rotational diffusion coefficient, $D_{\parallel}$, and the orientation of the probe with respect to the diffusion axis. The rigorous analysis of these data in terms of the uniaxial rotational diffusion model requires that the probe adopt a unique or narrow distribution of orientations with respect to the protein.

The most direct approach for addressing the question of the uniqueness of the labeling geometry and for determining the orientation of an exogenous probe relative to the membrane normal axis is to use a sample in which a known anisotropic distribution of membrane normal axes has been established. Spectroscopic data, obtained at selected sample orientations, can then be analyzed to determine the orientation of the probe. The analysis of the linear EPR spectra of nitroxide spin-labels in terms of the nitroxide orientational distribution in an ordered sample is well-established (Libertini et al., 1974; Burghardt & Thompson, 1985; Burghardt & French, 1989; Fajer, 1994). In addition, previous work has shown that intact erythrocytes can be oriented by flow (Hubbell & McConnell, 1969; Noji et al., 1981). Using the fatty acid spin-label, 5-nitroxyl stearate (5-NS), Hubbell and McConnell (1969) demonstrated by a comparison of the EPR spectra obtained with the flat cell at two orthogonal orientations relative to the external magnetic field that erythrocytes preferentially orient when flowing through an EPR flat cell. Bitbol and Leterrier (1982) have shown that the EPR spectra of 5-NS-labeled erythrocytes flowing through a flat cell can be reasonably modeled assuming a fraction of the cells are perfectly oriented biconcave disks with the remainder totally disordered. As an initial determination of the orientation of the nitroxide with respect to the membrane normal, the linear EPR spectra of [^{15}N,^{2}H$_{13}$]-SL-H$_2$DADS-maleimide-labeled band 3 in erythrocytes oriented by flow, obtained for two orthogonal sample orientations, have been simultaneously fit using the model of Bitbol and Leterrier (1982).

For 5-NS, the effective **A** and **g** tensors are axial, with the unique (*z*-) axis aligned perpendicular to the membrane surface (Libertini et al., 1969; Hubbell & McConnell, 1969; McConnell & McFarland, 1970). Thus, the orientation distribution of nitroxide *z*-axes, readily determined from linear EPR spectra, is equivalent to the membrane normal orientation distribution. Following Burghardt and co-workers (Burghardt & Thompson, 1985; Burghardt & French, 1989), the membrane normal orientation distribution for 5-NS-labeled erythrocytes oriented by flow has been determined as a linear combination of spherical harmonic basis functions. This orientation distribution has then been used to reanalyze the EPR spectra of [^{15}N,^{2}H$_{13}$]-SL-H$_2$DADS-maleimide-labeled band 3 in erythrocytes, allowing a second determination of the orientation of the nitroxide relative to the membrane normal.

The orientation of the nitroxide with respect to the membrane normal as determined in the present study from the linear EPR studies of oriented erythrocytes is nearly identical to the orientation of the nitroxide with respect to the uniaxial rotational diffusion axis as determined from previous ST-EPR studies (Hustedt & Beth, 1995). This confirms that the motion observed by ST-EPR studies of [^{15}N,^{2}H$_{13}$]-SL-H$_2$DADS-maleimide-labeled band 3 in intact erythrocytes is a rotation about the membrane normal. Portions of this work have been previously published as an abstract (Hustedt & Beth, 1994).

METHODS

Erythrocyte Preparation. All experiments were performed using intact erythrocytes isolated from venous blood freshly drawn from healthy adults and collected in heparinized Vacutainer (Becton Dickinson, Rutherford, NJ) tubes. Erythrocytes were washed free of plasma and other cells by three suspension, centrifugation, and aspiration cycles in 113 mM citrate buffer at pH 7.4. Unless otherwise noted, all operations were performed at 0−4 °C.

[^{15}N,^{2}H$_{13}$]-SL-H$_2$DADS-maleimide Labeling of Band 3 in Intact Erythrocytes. The synthesis of [^{15}N,^{2}H$_{13}$]-SL-H$_2$-DADS-maleimide is described by Scothorn et al. in the preceding paper. An aliquot of a 2 mM solution of [^{15}N,^{2}H$_{13}$]-SL-H$_2$DADS-maleimide, freshly dissolved in 113 mM citrate buffer at pH 7.4, was added to whole packed erythrocytes on ice to a final concentration of 28 nmol/mL of cells. After 1 h, the reaction was quenched by the addition of 10 volumes of 0.2% (w:v) bovine serum albumin (fraction V, Sigma Chemical Co., St. Louis, MO) in 113 mM citrate buffer solution at pH 7.4. After an additional 30 min on ice, the suspension was centrifuged for 10 min at 3000*g* and washed a second time with 0.2% bovine serum albumin and then twice with 113 mM citrate buffer at pH 7.4.

Labeling of Erythrocytes with [^{15}N,^{2}H$_{12}$]-5-NS. The [^{15}N,^{2}H$_{12}$]-5-nitroxylstearic acid spin-label (5-NS) was generously provided by Dr. J. Feix (Medical College of Wisconsin, Milwaukee, WI). An aliquot of a 1.5 mM solution of 5-NS in chloroform was placed in a glass test tube and the solvent evaporated under a gentle stream of nitrogen gas. Packed erythrocytes were then added, and the test tube was gently rotated and warmed by hand for 10 min. The 5-NS-labeled erythrocytes were then washed with 10 volumes of buffer. This procedure gave essentially complete incorporation of 5-NS into the erythrocyte membranes at a final concentration of 20 nmol/mL of cells.

Measurement of EPR Spectra. All EPR spectra were recorded on a Bruker ESP-300 spectrometer equiped with

an ER-4103 TM_{110} cavity and an ER-4111VT variable-temperature control unit. Linear V_1 EPR spectra were recorded using a 10 mW microwave observer power with a 100 kHz Zeeman modulation amplitude (peak-to-peak) of 1 G (5-NS) or 0.5 G (SL-H_2DADS-maleimide). The sample temperature was maintained by blowing nitrogen gas at the appropriate temperature through the front optical port of the cavity. The spectra of isotropically oriented erythrocytes were collected with samples in 50 μL disposable microsampling pipets (Scientific Products Division, Corning Glass Works, Corning, NY). The spectra of preferentially oriented erythrocytes were obtained by flowing erythrocytes through a modified WG-812 EPR flat cell (Wilmad Glass Co., Buena, NJ) with a 120 μm gap. Continuous flow of the erythrocytes was maintained with a Minipuls 2 peristaltic pump (Gilson Medical Electronics, Middleton, WI). The flow rate was maintained at approximately 0.2 mL/min. Higher rates of flow did not affect the EPR spectra. The EPR flat cell was placed in the cavity such that a vector pependicular to the face of the flat cell was aligned either perpendicular to the magnetic field (the conventional orientation) or parallel to it. After collection of the spectra at the two orientations, the percentage of hemolysis was determined from the amount of hemoglobin free in solution as detected by visible absorbance at 415 nm. For both the 5-NS- and SL-H_2DADS-maleimide-labeled samples, hemolysis was less than 2%.

Nonlinear Least Squares Analysis of EPR Spectra. All data analyses were performed by incorporating algorithms for calculating EPR spectra for various models into a general nonlinear least squares program which has the capability of simultaneous, global analysis of multiple data sets as previously described (Hustedt et al., 1993). Global χ^2 values were calculated with estimates of the uncertainty in the data obtained from the base line regions of the spectra.

Analysis of Linear EPR Spectra−Isotropic Label Distribution. In order to determine the rigid-limit **A** and **g** tensors and line width parameters, which are needed to analyze the EPR spectra obtained for oriented erythrocytes, the linear EPR spectra of isotropically oriented cells were fit using nonlinear least squares analysis based on the Marquardt−Levenberg algorithm as described by Hustedt et al. (1993). In the absence of a precise determination of the spectrometer microwave frequency, the isotropic g value, $\bar{g} = {}^1/_3(g_{xx} + g_{yy} + g_{zz})$, has been assumed to be 2.0055. To fully account for various line width effects, the Lorentzian line width, Γ, was treated, when necessary, as both manifold (nuclear spin state)- and orientation-dependent,

$$\Gamma(m_I;\theta,\phi) = \Gamma_0(m_I) + \Gamma_\theta(m_I)(1 - 3\cos^2\theta) + \Gamma_\phi(m_I)(\sin^2\theta)(\cos^2\phi - \sin^2\phi) \quad (1)$$

where θ and ϕ are the polar angles which determine the orientation of the coincident **A** and **g** tensors relative to the magnetic field and m_I is the ^{15}N nuclear spin state. The simulation was convolved, when necessary, with a Gaussian of manifold-dependent width $\sigma(m_I)$ to account for inhomogeneous broadening due to weakly coupled deuterons.

Analysis of Linear EPR Spectra-Oriented Erythrocytes. In the high-field approximation, the diagonalized nitroxide spin Hamiltonian is given by

$$\hat{H} = (\beta_e/\hbar)g_{eff}HS_z - \gamma_e A_{eff} I_z S_z \quad (2)$$

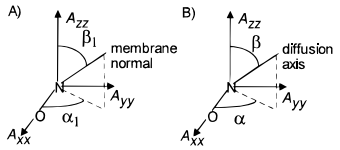

FIGURE 1: (A) Orientation of the nitroxide **A** tensor with respect to the membrane normal vector as determined by the angles α_1 and β_1. The nitroxide **A** and **g** tensors are assumed to be coincident. (B) Orientation of the nitroxide **A** tensor with respect to the uniaxial rotational diffusion axis as determined by the angles α and β.

where I_z and S_z are spin angular-momentum operators of the ^{15}N nucleus and the electron, respectively, γ_e is the electron gyromagnetic ratio, β_e is the Bohr magneton, and H is the applied magnetic field. The factors g_{eff} and A_{eff} are determined by the orientation of the nitroxide with respect to the magnetic field. For a nitroxide oriented such that the magnetic field is aligned with its z-axis, the **A** tensor ($\mathbf{A}_d$) is diagonal. Equation 3 gives the elements of the **A** tensor for an arbitrary orientation determined by the orientation of the nitroxide with respect to the membrane normal (Ω_1), the orientation of the membrane normal with respect to the flat cell (Ω_2), and the orientation of the flat cell in the magnetic field (Ω_3).

$$\mathbf{A} = \mathbf{R}_3(\Omega_3)\mathbf{R}_2(\Omega_2)\mathbf{R}_1(\Omega_1)\mathbf{A}_d\mathbf{R}_1^{-1}(\Omega_1)\mathbf{R}_2^{-1}(\Omega_2)\mathbf{R}_3^{-1}(\Omega_3) \quad (3)$$

$$\mathbf{R}(\Omega) = \mathbf{R}(\gamma,\beta,\alpha) = \mathbf{R}_z(\gamma)\mathbf{R}_y(\beta)\mathbf{R}_z(\alpha)$$

$$\mathbf{R}_z(\alpha) = \begin{bmatrix} \cos\alpha & \sin\alpha & 0 \\ -\sin\alpha & \cos\alpha & 0 \\ 0 & 0 & 1 \end{bmatrix}$$

$$\mathbf{R}_y(\beta) = \begin{bmatrix} \cos\beta & 0 & -\sin\beta \\ 0 & 1 & 0 \\ \sin\beta & 0 & \cos\beta \end{bmatrix}$$

$$\mathbf{R}_z(\gamma) = \begin{bmatrix} \cos\gamma & \sin\gamma & 0 \\ -\sin\gamma & \cos\gamma & 0 \\ 0 & 0 & 1 \end{bmatrix}$$

An equivalent expression can be written for the **g** tensor, which is assumed to be coincident with the **A** tensor.

The angles α_1 and β_1 determine the orientation of the nitroxide with respect to the membrane normal as shown in Figure 1A. The angle between the membrane normal axis and the z-axis of the nitroxide is defined by β_1. For a nonzero β_1, the angle α_1 determines the projection of the membrane normal onto the $x-y$ plane of the nitroxide. Experimental sensitivity to α_1 is limited by the small nonaxial character of the nitroxide **A** tensor and the minor influence of the **g** tensor at X-band (approximately 10 GHz). The angle γ_1 corresponds to a rotation of the nitroxide (or the protein to which it is attached) about the membrane normal. It is the angle which governs the uniaxial rotational diffusion of the protein about the membrane normal. Since these motions are expected to occur on a microsecond or slower time scale and linear EPR is not sensitive to motions on this time scale, γ_1 takes on a static, uniform distribution between 0 and 2π. The rotation by α_2 is equivalent to that by γ_1 and can be disregarded. The angles β_2 and γ_2 determine the orientation of the membrane normal with respect to the sample. Two different treatments of these angles are discussed below. The angle α_3 is equivalent to γ_2 and is

disregarded. The angle β_3 determines the orientation of the sample in the magnetic field. For $\beta_3 = 0$, the membrane normal vector at the center of a perfectly aligned erythrocyte is parallel to the magnetic field. For $\beta_3 = \pi/2$, such a vector is perpendicular to the magnetic field.

The values of A_{eff} and g_{eff} are given by (Balasubramanian & Dalton, 1979)

$$A_{\text{eff}} = \sqrt{(A_{1,3})^2 + (A_{2,3})^2 + (A_{3,3})^2} \qquad (4)$$

$$g_{\text{eff}} = g_{3,3}$$

with

$$A_{i,3} = \sum_{j,k,l,m,n} (R_3)_{ij}(R_2)_{jk}(R_3)_{kl}(A_d)_{ll}(R_1^{-1})_{lm}(R_2^{-1})_{mn}(R_3^{-1})_{3n} \qquad (5)$$

$$= \sum_{j,k,l,m,n} (R_3)_{ij}(R_2)_{jk}(R_3)_{kl}(A_d)_{ll}(R_1)_{ml}(R_2)_{nm}(R_3)_{3n}$$

and an equivalent expression for the **g** tensor elements. From eqs 4 and 5, it can be shown that the angle γ_3 has no effect on the values of g_{eff} and A_{eff} and can be disregarded. Likewise, for $\beta_3 = 0$, γ_2 can be disregarded.

For a fixed microwave frequency, ω_0, and a given nitroxide nitrogen spin state, m_{I}, the EPR spectrum of a nitroxide at a particular orientation is given by the first derivative Lorentzian line shape

$$\nu(H;\beta_3,\gamma_2,\beta_2,\gamma_1,\beta_1,\alpha_1;m_{\text{I}}) = \frac{(H - H_{\text{res}})\Gamma}{[(H - H_{\text{res}})^2 + \Gamma^2]^2} \qquad (6)$$

where Γ is the Lorentzian line width and

$$H_{\text{res}} = \frac{\omega_0 - m_{\text{I}}\gamma_e A_{\text{eff}}}{g_{\text{eff}}} \qquad (7)$$

The total EPR spectrum is given by the sum of the two manifolds, corresponding to the two possible ^{15}N nuclear spin states, each of which is obtained by an integral over all possible orientations. For the perpendicular orientation, $\beta_3 = \pi/2$, the calculation is a triple integral over γ_1, β_2, and γ_2.

$$V(H;\beta_3,\beta_1,\alpha_1) = \sum_{m_{\text{I}}=-1/2}^{+1/2} \int_0^{2\pi}\int_0^{\pi}\int_0^{2\pi} \nu(H;\beta_3,\gamma_2,\beta_2,\gamma_1,\beta_1,\alpha_1;m_{\text{I}}) N(\beta_2,\gamma_2) \sin\beta_2 \, d\gamma_1 \, d\beta_2 \, d\gamma_2 \qquad (8)$$

where $N(\beta_2,\gamma_2)$ is the probability that a membrane normal is oriented at angles β_2 and γ_2 with respect to the sample. For the parallel orientation, $\beta_3 = 0$, the calculation is a double integral over γ_1 and β_2.

Partially Oriented Biconcave Disks. The integration over the angle γ_1 in eq 8 is independent of both the cell shape and the orientational distribution of cells within the sample. Let

$$\nu'(H;\beta_3,\gamma_2,\beta_2,\beta_1,\alpha_1;m_{\text{I}}) = \int_0^{2\pi} \nu(H;\beta_3,\gamma_2,\beta_2,\gamma_1,\beta_1,\alpha_1;m_{\text{I}}) \, d\gamma_1 \qquad (9)$$

For an erythrocyte perfectly aligned within the flat cell, the orientation of the membrane normal with respect to the flat cell is equivalent to the orientation of the membrane normal with respect to the axis frame fixed within the erythrocyte whose z-axis is the C_∞ symmetry axis of the erythrocyte. The total EPR spectrum can be obtained as the sum of integrals over the erythrocyte surface.

$$V(H;\beta_3,\beta_1,\alpha_1) = \sum_{m_{\text{I}}=-1/2}^{+1/2} \int_s \nu'(H;m_{\text{I}}) \, dS \qquad (10)$$

The surface integrals can be transformed into integrals over a circular region in the $x-y$ plane of the erythrocyte (Marsden & Tromba, 1976),

$$V(H;\beta_3,\beta_1,\alpha_1) = \sum_{m_{\text{I}}=-1/2}^{+1/2} \int\int \frac{\nu'(H;m_{\text{I}})}{\cos\beta_2} \, dx \, dy \qquad (11)$$

with

$$\cos\beta_2 = \left[\left(\frac{\partial z}{\partial x}\right)^2 + \left(\frac{\partial z}{\partial y}\right)^2 + 1\right]^{-1/2} \qquad (12)$$

Evans and Fung (1972), using interference microscopy, have determined a parameterized function which describes the biconcave disk shape of the typical erythrocyte.

$$z(r) = {}^1/_2[1 - (r/R_0)^2]^{1/2}[C_0 + C_2(r/R_0)^2 + C_4(r/R_0)^4] \qquad (13)$$

where

$$r = \sqrt{x^2 + y^2}, \quad R_0 = 3.91\ \mu\text{m}, \quad C_0 = 0.81\ \mu\text{m}, \quad C_2 = 7.83\ \mu\text{m}, \quad C_4 = -4.39\ \mu\text{m}$$

Transforming the integrals in eq 11 to cylindrical coordinates, $x = r\cos\gamma_2$ and $y = r\sin\gamma_2$, and backsubstituting for ν' gives

$$V(H;\beta_3,\beta_1,\alpha_1) = \sum_{m_{\text{I}}=-1/2}^{+1/2} \int_0^{2\pi}\int_0^{R_0}\int_0^{2\pi} \frac{\nu(H;\beta_3,\gamma_2,\beta_2(r),\gamma_1,\beta_1,\alpha_1;m_{\text{I}})}{\cos\beta_2\,(r)} r \, d\gamma_1 \, dr \, d\gamma_2 \qquad (14)$$

where

$$\cos\beta_2\,(r) = \left[\left(\frac{\partial z}{\partial r}\right)^2 + 1\right]^{-1/2} \qquad (15)$$

or

$$\beta_2(r) = \arccos\left\{\left[\left(\frac{\partial z}{\partial r}\right)^2 + 1\right]^{-1/2}\right\} \qquad (16)$$

The integrals in eq 14 were solved numerically as sums at discrete, equally spaced values of γ_1, r, and γ_2. Typically, 128 values for each variable were used. No significant change in the simulated spectra was seen if more values were used. To account for imperfectly aligned erythrocytes and variations in cell shape, a variable fraction, f, of the cells was assumed to be isotropically oriented or, equivalently, spherically shaped. The EPR spectrum of such erythrocytes can be conveniently calculated using this same algorithm

with $R_0 = 1$, $C_0 = 2$, and $C_2 = C_4 = 0$. For the nonlinear least squares analysis of data, this model was incorporated into a previously described computer program (Hustedt et al., 1993).

Model-Independent Determination of Orientational Distribution. Burghardt and co-workers (Burghardt & Thompson, 1985; Burghardt & French, 1989) have developed methods for the analysis of the EPR spectra of ordered, spin-labeled biological systems in terms of a model-independent determination of the orientational distribution. The membrane normal orientational distribution function, $N(\beta_2,\gamma_2)$, can be expanded in terms of the complete, orthonormal set of spherical harmonics.

$$N(\beta_2,\gamma_2) = \sum_{l=0}^{\infty} \sum_{m=-l}^{+l} \alpha_{l,m} Y_{l,m}(\beta_2,\gamma_2) \qquad (17)$$

Certain symmetry relations apply which limit the sensitivity of EPR spectra to specific terms in eq 17 (Burghardt & French, 1989). For the case of the 5-NS label, where $\alpha_1 = \beta_1 = \gamma_1 = 0$, and for the sample orientations employed in this work, $\beta_3 = 0$ and $\beta_3 = \pi/2$, the following symmetry relations apply to the EPR spectra corresponding to particular orienations.

$$\nu(H;\beta_3 = 0 \text{ or } \pi/2,\gamma_2,\beta_2,\gamma_1 = \beta_1 = \alpha_1 = 0;m_I) = \qquad (18)$$

$$\nu(H;\beta_3 = 0 \text{ or } \pi/2,\gamma_2,\pi-\beta_2,\gamma_1 = \beta_1 = \alpha_1 = 0;m_I) =$$

$$\nu(H;\beta_3 = 0 \text{ or } \pi/2,\pi+\gamma_2,\beta_2,\gamma_1 = \beta_1 = \alpha_1 = 0;m_I)$$

As a result, the contribution of a particular spherical harmonic to the total EPR spectrum

$$\int_0^{2\pi}\int_0^{\pi}\int_0^{2\pi} \nu(H;\beta_3,\gamma_2,\beta_2,\gamma_1,\beta_1,\alpha_1;m_I) Y_{l,m}(\beta_2,\gamma_2) \sin\beta_2 \, d\gamma_1 \, d\beta_2 \, d\gamma_2 \qquad (19)$$

will be zero if either

$$Y_{l,m}(\beta_2,\gamma_2) = -Y_{l,m}(\pi-\beta_2,\gamma_2) \qquad (20)$$

or

$$Y_{l,m}(\beta_2,\gamma_2) = -Y_{l,m}(\beta_2,\pi+\gamma_2) \qquad (21)$$

Thus, the extent of the contribution of the $Y_{l,m}$ which satisfy eq 20 or 21 to the actual orientational distribution, $N(\beta_2,\gamma_2)$, cannot be determined in the experiments performed in this study. These considerations restrict both l and m to even values. A final symmetry relation,

$$\nu(H;\beta_3 = 0 \text{ or } \pi/2,\gamma_2,\beta_2,\gamma_1 = \beta_1 = \alpha_1 = 0;m_I) = \qquad (22)$$

$$\nu(H;\beta_3 = 0 \text{ or } \pi/2,\pi-\gamma_2,\beta_2,\gamma_1 = \beta_1 = \alpha_1 = 0;m_I)$$

guarantees that only the real, $\cos(m\phi)$, terms of the spherical harmonics will contribute to the observed EPR spectra. With the further restrictions that $N(\beta_2,\gamma_2)$ be pure real and normalized, eq 17 is reduced to

$$N(\beta_2,\gamma_2) = \frac{1}{\sqrt{4\pi}} Y_{0,0} + \sum_{l=2,4,\ldots}^{\infty} [a_{l,0} Y_{l,0}(\beta_2,\gamma_2) + \sum_{m=2,4,\ldots}^{l} a_{l,m}(Y_{l,m}+Y_{l,-m})(\beta_2,\gamma_2)] \qquad (23)$$

It is important to note that these restrictions are on the sensitivity of EPR at the two sample orientations employed and not on the true nature of $N(\beta_2,\gamma_2)$. In one important case, however, it is expected that $N(\beta_2,\gamma_2)$ should be independent of an inversion through the sample plane, i.e. $N(\beta_2,\gamma_2) = N(\pi-\beta_2,\gamma_2)$, which implies that spherical harmonics which satisfy eq 20 do not contribute to the true orientational distribution.

The total EPR spectrum, averaged over the entire sample, is given by eq 8, with $N(\beta_2,\gamma_2)$ as given by eq 23. The integrals were solved numerically as sums at equally spaced values of the angles γ_1, β_2, and γ_2 with the sums over l and m truncated at finite values of $l = l_{max}$ and $m = m_{max}$. For 5-NS-labeled cells, the angles α_1 and β_1 are known to have time-averaged values of zero (Libertini et al., 1969; Hubbell & McConnel, 1969; McConnell & McFarland, 1970) and β_3 is the known orientation of the sample within the magnetic field. In this case, the analysis of data is a question of determining the linear coefficients $a_{l,m}$ of eq 23. We have, nonetheless, incorporated this model into a generalized nonlinear least squares analysis program (Hustedt et al., 1993) for two reasons. The first is the ease with which it could be used to simultaneously analyze the two data sets obtained at different sample orientations, and the second is the need to perform nonlinear analysis to fit the SL-H_2-DADS-maleimide data in terms of the angles α_1 and β_1 for a fixed set of $a_{l,m}$. Results from nonlinear least squares analysis of the two data sets individually were essentially identical to those obtained by linear least squares analysis using a singular value decomposition algorithm (Press et al., 1986).

RESULTS

EPR Spectrum of [^{15}N,$^{2}H_{13}$]-SL-H_2DADS-maleimide-Labeled Band 3 in Isotropically Oriented Erythrocytes. Figure 2 shows the linear EPR spectrum (dots) of [^{15}N,$^{2}H_{13}$]-SL-H_2DADS-maleimide-labeled band 3 in intact erythrocytes in a 50 μL capillary at 20 °C. The spectrum was fit to a rigid-limit powder pattern (solid line) in order to determine the nitroxide **A** and **g** tensors and line width parameters which were then used to fit the EPR spectra of flow-oriented erythrocytes. The fit to the data is excellent except for a small mismatch in the region from approximately −20 to −15 G (relative to the center field value of ≈3500 G) which is due to the presence of a small (<1%) percentage of partially immobilized label not bound to band 3. This small percentage of label cannot be removed by additional washings with buffer and is presumably covalently bound to other erythrocyte components, perhaps to membrane phospholipid. This small region from −20 to −15 G was not included in the calculation of χ^2 in the nonlinear least squares analysis of the data. The high-field manifold of the partially immobilized component is also present from approximately +5 to +15 G but did not have an influence on the analysis. The fit was not significantly improved by using manifold-dependent or anisotropic line widths. Both of these results

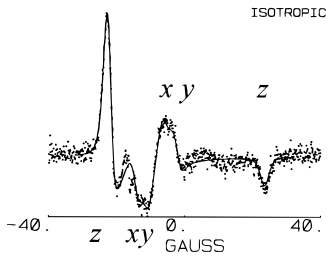

FIGURE 2: EPR spectrum (dots) of [^{15}N,^{2}H$_{13}$]-SL-H$_2$DADS-maleimide-labeled band 3 in erythrocytes in a 50 μL capillary at 20 °C. The overlaid fit (solid line) was calculated assuming a rigid-limit isotropic distribution of nitroxide orientations. The best fit parameters were as follows: $g_{xx} = 2.00848$, $g_{yy} = 2.00596$, $g_{zz} = 2.00206$, $A_{xx} = 7.98$ G, $A_{yy} = 8.19$ G, $A_{zz} = 46.17$ G, $\Gamma_0(-1/2) = \Gamma_0(+1/2) = 0.75$ G, $\Gamma_\theta(-1/2) = \Gamma_\theta(+1/2) = 0.0$, $\Gamma_\phi(-1/2) = \Gamma_\phi(+1/2) = 0.0$, and $\sigma(-1/2) = \sigma(+1/2) = 0.94$ G. The labels *x*, *y*, and *z* indicate the approximate field positions (turning points) in the two manifolds of the EPR spectrum where the resonance condition is met for nitroxides whose *x*-, *y*-, or *z*-axes, respectively, are aligned with the DC magnetic field.

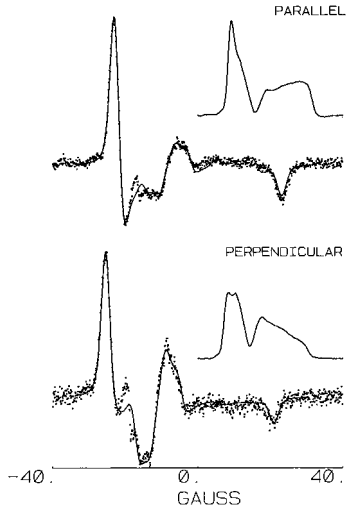

FIGURE 3: EPR spectra (dots) of [^{15}N,^{2}H$_{13}$]-SL-H$_2$DADS-maleimide-labeled band 3 in erythrocytes flowing through an EPR flat cell at 20 °C at the two orthogonal orientations of the flat cell. The integrated spectra (inset) clearly show the dependence of the spectra on sample orientation. The overlaid fits (solid lines) were obtained by a simultaneous nonlinear least squares analysis of both data sets assuming a fraction, *f*, of the cells are perfectly oriented biconcave disks with the remainder isotropically distributed. The best fit parameters were as follows: $f = 0.60$, $\alpha_1 = 58°$, and $\beta_1 = 36°$. The **A** and **g** tensor elements and line widths were those obtained for the powder pattern fit in Figure 2.

are consistent with a probe which is highly immobile on the linear EPR time scale ($\tau \geq 1$ μs), and therefore a probe which is tightly coupled to band 3. Furthermore, a comparison of this spectrum, obtained at 20 °C, with those obtained at 6 or 37 °C (data not shown) demonstrates that there is very little temperature dependence of the linear EPR spectra and, thus, there is little, if any, temperature-sensitive motion (on the linear EPR time scale) of the probe independent of band 3.

To confirm that erythrocytes are isotropically orientated in a 50 μL capillary, a sample of [^{15}N,^{2}H$_{13}$]-SL-H$_2$DADS-maleimide-labeled band 3 in intact erythrocytes was placed in a ≈1 cm section of capillary tube and positioned in the EPR cavity such that the long axis of the sample tube was parallel to the external magnetic field. The EPR spectrum obtained from this sample (data not shown) did not noticeably differ from that in Figure 2, where the sample was oriented perpendicular to the magnetic field. The lack of any dependence of the EPR spectra on sample orientation demonstrates that the erythrocytes are isotropically oriented in a 50 μL capillary.

EPR Spectra of [^{15}N,^{2}H$_{13}$]-SL-H$_2$DADS-maleimide-Labeled Band 3 in Erythrocytes Preferentially Oriented by Flow through an EPR Flat Cell. Figure 3 shows the linear EPR spectra (dots) of [^{15}N,^{2}H$_{13}$]-SL-H$_2$DADS-maleimide-labeled band 3 in intact erythrocytes flowing through an EPR flat cell at 20 °C. The sample is oriented such that a vector perpendicular to the face of the flat cell is aligned either parallel or perpendicular to the magnetic field. It is evident that there is a relative increase in intensity at the *z*-turning point for the parallel orientation and a relative increase in intensity at the *x*- and *y*-turning points for the perpendicular orientation (see Figure 2 for definition of turning points). The sample orientation dependence of these EPR spectra is even more obvious in the integrated spectra shown as insets in Figure 3. These observations mirror those observed using the fatty acid spin-label, 5-NS (see Figure 5 below), for which it is known that the effective nitroxide *z*-axis is aligned with the membrane normal axis. These qualitative observations indicate that the nitroxide *z*-axis of SL-H$_2$DADS-maleimide bound to band 3 is more nearly aligned with the membrane normal axis than with the membrane surface.

The spectra in Figure 3 were initially analyzed according to the model of Bitbol and Leterrier (1982). A variable fraction of the cells, *f*, is assumed to be perfectly aligned biconcave disks whose shape is given by eq 13. In order to account for the variation in cell shape and the lack of perfect orientational order, the remainder of the cells are assumed to be spherical or, equivalently, randomly oriented within the flat cell. The fits (solid lines) overlaid on the data in Figure 3 were obtained by simultaneous least squares analysis of both data sets, using the **A** and **g** tensors and line width parameters obtained from the analysis of the data in Figure 2. The parameters varied were the angles which determine the orientation of the nitroxide with respect to the membrane normal, α_1 and β_1, and the fraction of isotropically distributed cells. For both data sets, the relative intensities at the *z*-turning point versus the *x*- and *y*-turning points have been matched by the calculated spectra. Again, the largest deviations of the fits from the data sets, in the regions from approximately −20 to −15 G, are due to the presence of a very small percentage of label not bound to band 3, and these regions were not included in the fits. The value of β_1 obtained, 36°, is consistent with a net increase in intensity at the *z*-turning point for the parallel orientation.

An attempt was made to determine if there were any significant temperature effects on nitroxide orientation or the degree of erythrocyte orientation. Equivalent experiments were performed with labeled erythrocytes, precooled or preheated to the appropriate temperature, flowing through the flat cell with the cavity temperature maintained at 6 or 37 °C. No significant temperature dependence of the EPR spectra was observed (data not shown).

EPR Spectrum of 5-NS-Labeled, Isotropically Oriented Erythrocytes. In order to obtain an independent estimate of the degree of orientational order and the actual distribution of membrane normal vectors for erythrocytes oriented by flow, an equivalent set of experiments was performed on erythrocytes labeled with the spin-labeled fatty acid 5-NS.

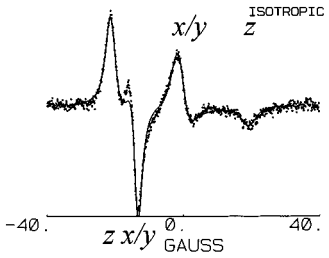

FIGURE 4: EPR spectrum (dots) of [^{15}N,^{2}H$_{12}$]-5-NS-labeled erythrocytes in a 50 μL capillary at 20 °C. The overlaid fit (solid line) was calculated assuming a rigid-limit isotropic distribution of nitroxide orientations and axial **A** and **g** tensors. The best fit parameters were as follows: $g_{xx} = g_{yy} = 2.00671$, $g_{zz} = 2.00307$, $A_{xx} = A_{yy} = 12.99$ G, $A_{zz} = 40.58$ G, $\Gamma_0(-1/2) = 1.61$ G, $\Gamma_0(+1/2) = 1.52$ G, $\Gamma_\theta(-1/2) = -0.10$ G, $\Gamma_\theta(+1/2) = -0.07$ G, $\Gamma_\phi(-1/2) = \Gamma_\phi(+1/2) = 0.0$, $\sigma(-1/2) = 0.44$ G, and $\sigma(+1/2) = 1.31$ G. The labels *x*, *y*, and *z* indicate the approximate positions of the turning points in the two manifolds of the EPR spectrum. The *x* and *y* turning points are equivalent because the rapid rotation of the 5-NS about the membrane normal axis produces axial **A** and **g** tensors.

Fatty acids undergo rapid, restricted motion within a bilayer. Nevertheless, the EPR spectrum of a 5-NS in a lipid bilayer can be fit as a rigid-limit spectrum using motionally averaged **A** and **g** tensors. Because the motion of the spin-label is symmetric about an axis perpendicular to the membrane, the motionally averaged **A** and **g** tensors are axial with the *z*-axis of the tensors parallel to the membrane normal (Libertini et al., 1969; Hubbell & McConnell, 1969; McConnell & McFarland, 1970).

Figure 4 shows the linear EPR spectrum (dots) of 5-NS-labeled erythrocytes in a 50 μL capillary at 20 °C. The distribution of nitroxide orientations is taken to be isotropic, and the spectrum is fit to a rigid-limit powder pattern spectrum (solid line) to determine the motionally averaged **A** and **g** tensors and line width parameters. For the fit shown, the **A** and **g** tensors were constrained to be axial. However, no significant improvement in χ^2 was obtained by relaxing this constraint. On the other hand, the fit was significantly improved by including manifold-dependent and anisotropic line width terms. These results are entirely consistent with a nitroxide undergoing rapid, symmetric rotation about a single axis.

EPR Spectra of [^{15}N,^{2}H$_{12}$]-5-NS-Labeled Erythrocytes Preferentially Oriented by Flow through an EPR Flat Cell. Figure 5 shows the linear EPR spectra (dots) of [^{15}N,^{2}H$_{12}$]-5-NS-labeled erythrocytes at 20 °C flowing through an EPR flat cell oriented such that a vector perpendicular to the face of the flat cell is aligned either parallel or perpendicular to the magnetic field. These spectra clearly show the relative increase in the intensity at the *z*-turning points for the parallel orientation and the relative increase in the intensity at the *x*- and *y*-turning points for the perpendicular orientation which are characteristic of a lipid spin-label whose *z*-axis is aligned with the membrane normal axis in flow-oriented erythrocytes (see Figure 4 for definition of turning points). In order to compare with the results obtained above, these spectra were initially fit to the model of Bitbol and Letterier (1982). Assuming that $\alpha_1 = \beta_1 = 0°$ for the 5-NS label (Libertini et al., 1969; Hubbell & McConnell, 1969; McConnell & McFarland, 1970), the single unknown is the fraction of perfectly oriented biconcave disks. The best fit value obtained was $f = 0.69$ (fits not shown) which was in reasonable agreement with the value obtained above ($f = 0.60$) for the [^{15}N,^{2}H$_{13}$]-SL-H$_2$DADS-maleimide label. These values are both slightly higher than the largest values, $f \approx 0.5$, obtained by Bitbol and Leterrier (1982) under similar conditions except for their use of a flat cell with a standard 300 μm gap.

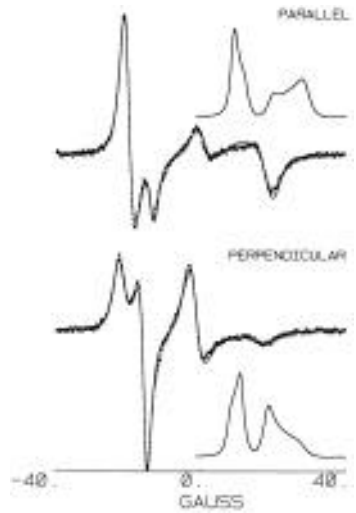

FIGURE 5: EPR spectra (dots) of [^{15}N,^{2}H$_{12}$]-5-NS-labeled erythrocytes flowing through an EPR flat cell at 20 °C. The integrated spectra (inset) clearly show the dependence of the spectra on sample orientation. The overlaid fits (solid lines) were obtained by a simultaneous nonlinear least squares analysis of both data sets. The fit parameters are the coefficients, $a_{l,m}$, which determine the membrane normal orientation distribution according to eq 23. The fit shown corresponds to $l_{max} = 14$ and $m_{max} = 2$; no significant improvement in fit was seen for higher values. The **A** and **g** tensor elements and line widths were those obtained for the powder pattern fit in Figure 4.

In order to obtain a model-independent measure of the orientational distribution of membrane normals for erythrocytes flowing through a flat cell, the spectra in Figure 5 were fit to eqs 8 and 23. Assuming that $\alpha_1 = \beta_1 = 0°$ for the 5-NS label (Libertini et al., 1969; Hubbell & McConnell, 1969; McConnell & McFarland, 1970), the unknown parameters are the set of $a_{l,m}$ values. Terms up to $l_{max} = 14$ and $m_{max} = 2$ were included in the fits (solid lines) shown in Figure 5. Inclusion of additional terms, particularly higher *l* values, did slightly improve the global χ^2. However, when these additional terms were included, $N(\beta_2,\gamma_2)$ became highly oscillatory and took on unrealistic, negative values.

Reanalysis of the EPR Spectra of [^{15}N,^{2}H$_{13}$]-SL-H$_2$DADS-maleimide-Labeled Band 3 in Preferentially Oriented Erythrocytes. Figure 6 shows the same data as in Figure 3, the linear EPR spectra of [^{15}N,^{2}H$_{13}$]-SL-H$_2$DADS-maleimide-labeled band 3 in erythrocytes flowing through an EPR flat cell at 20 °C. Superimposed on the data (dots) are fits (solid lines) using the distribution of membrane normals, $N(\beta_2,\gamma_2)$, obtained in Figure 5 using the fatty acid spin-label. Simultaneous nonlinear least squares analysis of these two spectra gave best fit values of $\alpha_1 = 63°$ and $\beta_1 = 37°$.

The global χ^2 value obtained using a model-independent membrane normal orientation distribution, $\chi^2 = 1.45$, is slightly improved compared to that obtained using the model of Bitbol and Leterrier (1982), $\chi^2 = 1.51$. At the same time, the orientations determined by the two different approaches are not significantly different, $\alpha_1 = 63°$ and $\beta_1 = 37°$ versus $\alpha_1 = 58°$ and $\beta_1 = 36°$. This strongly suggests that the orientation determined is correct and that both models used

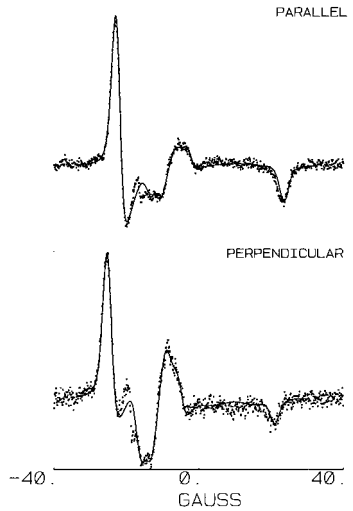

FIGURE 6: EPR spectra (dots) of [^{15}N,^{2}H$_{13}$]-SL-H$_2$DADS-maleimide-labeled band 3 in erythrocytes flowing through an EPR flat cell at 20 °C (same data as in Figure 3). The overlaid fits (solid lines) were obtained by a simultaneous nonlinear least squares analysis of both data sets using the membrane normal orientation distribution, $N(\beta_2,\gamma_2)$, obtained in Figure 5. The best fit angles obtained were as follows: $\alpha_1 = 61°$ and $\beta_1 = 37°$. The **A** and **g** tensor elements and line widths were those obtained from the powder pattern fit in Figure 3.

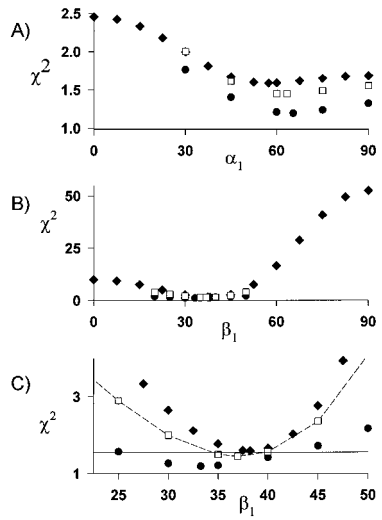

FIGURE 7: χ^2 surfaces for (A) α_1 and (B) β_1, and (C) an expanded view for β_1, obtained from the least squares analysis of the data in Figure 6. The symbols used are as follows: χ^2 surface for the fit to the EPR spectrum obtained for the parallel orientation alone (filled diamonds), χ^2 surface for the fit to the EPR spectrum obtained for the perpendicular orientation alone (filled circles), and χ^2 surface for the simultaneous fits to the EPR spectrum obtained for the parallel and perpendicular orientations (open squares). The horizontal line shows the χ^2 value defining the 90% confidence level for the determination of β_1 (Beechem et al., 1991).

give reasonable estimates of the membrane normal orientation distribution.

Figure 7 shows the χ^2 surfaces which are generated, using the model-free approach, by holding one angle at a fixed value and minimizing χ^2 by varying the other. The χ^2 curve for α_1 is rather flat for $\alpha_1 \geq 45°$, leading to a rather high uncertainty in this angle. This is to be expected given the fairly small value of β_1 (χ^2 would be independent of α_1 for $\beta_1 = 0°$) and the relatively small $x-y$ anisotropy of linear EPR spectra recorded at the X-band. For $\beta_1 \neq 0°$, α_1 determines the orientation of the nitroxide x- and y-axes relative to the membrane normal (Beth & Robinson, 1989). Conversely, the χ^2 surface for β_1 is quite steep due to the comparatively large $z-x$ and $z-y$ anisotropies. As shown in the expanded view in Figure 7, β_1 was determined to within approximately 5° at the 90% confidence level.

DISCUSSION

The potential for gaining detailed insights into various protein−protein and protein−lipid interactions involving membrane proteins has provided a strong impetus for the development and refinement, during the previous two decades, of methods for the quantification of their rotational dynamics. Early work [e.g. Hyde and Dalton (1972), Thomas and McConnell (1974), and Thomas et al. (1976)] demonstrated that ST-EPR spectroscopy, employing nitroxide spin-labels, provides high sensitivity to rotational motions in the micro- to millisecond time window which is the range expected for the global rotational diffusion of intrinsic membrane proteins. Numerous ST-EPR studies of membrane protein rotational dynamics have been reported [for reviews, see Thomas (1985, 1986)], including spin-labeled band 3 (Sakaki et al., 1982; Willingham & Gaffney, 1983; Beth et al., 1986; Anjaneyulu et al., 1988; Cobb et al., 1990).

The work described here and in a previous report (Hustedt & Beth, 1995) was undertaken with the long term goal of elucidating details of the rotational dynamics of band 3 through careful analysis of ST-EPR data. The motivation for the development of improved computational approaches (Hustedt & Beth, 1995) for the rigorous analysis of experimental ST-EPR spectra of molecules undergoing anisotropic rotational diffusion stems from early theoretical work (Beth et al., 1983) and experimental (Gaffney, 1979; Delmelle et al., 1980; Johnson et al., 1982; Fajer & Marsh, 1983) work which demonstrated that ST-EPR line shapes are highly sensitive to the diffusion model (i.e. isotropic, axial, or uniaxial), the rates of rotational diffusion, and the orientation of the spin-label relative to a unique diffusion axis. These same considerations have motivated the development and characterization of a band 3-specific spin-label which adopts a unique and definable orientation relative to band 3 and which will serve as a reliable reporter of the global rotational dynamics of band 3. The principal goal of this report is to determine the suitability of SL-H$_2$DADS-maleimide as a reporter for the global rotational dynamics of band 3. To meet this goal, it is necessary to determine the orientation of the nitroxide moiety of SL-H$_2$DADS-maleimide bound to band 3 in intact erythrocytes and to assess the extent to which the nitroxide does adopt a unique orientation.

Determination of the Orientation of SL-H$_2$DADS-maleimide Relative to the Membrane Normal Axis. Studies have been carried out to obtain the angles α_1 and β_1 which determine the orientation of the nitroxide moiety of SL-H$_2$-DADS-maleimide relative to the membrane normal axis (Figure 1A) of an intact erythrocyte by the analysis of linear EPR data collected from erythrocytes oriented by flow. It is important to emphasize that the linear EPR spectra are not sensitive to motions on the microsecond time scale, or slower. Therefore, linear EPR spectra of SL-H$_2$DADS-maleimide bound to band 3 in intact erythrocytes directly measure the nitroxide orientation distribution relative to the external

magnetic field. A determination of the orientation of the nitroxide relative to the membrane normal axis can be made if an anisotropic membrane normal orientational distribution can be created. Such an anisotropic membrane normal orientational distribution has been induced by orienting erythrocytes by flow through an EPR flat cell.

Two different approaches have been employed to determine the angles α_1 and β_1 from linear EPR spectra obtained from SL-H_2DADS-maleimide-labeled band 3 in intact erythrocytes oriented by flow through an EPR flat cell. In the first approach, spectra obtained at two different sample orientations were analyzed using a model of the erythrocyte orientational distribution first employed by Bitbol and Leterrier (1982). Previous work by Bitbol and Leterrier (1982) has shown that the membrane orientation distribution for 5-NS-labeled erythrocytes could be modeled in terms of a population of biconcave disks perfectly aligned with the flat cell surface and a second population of spherical cells or, equivalently, isotropically oriented cells. Simultaneous nonlinear least squares analysis of the spectra resulted in excellent agreement with experiment as shown by the fits superimposed on the data in Figure 3.

In the application of the model of Bitbol and Leterrier (1982), it has been assumed that all of the perfectly aligned cells have the same shape and that this shape is the same as that reported for static cells. However, Evans and Fung (1972) observed considerable variability in cell shape parameters. Furthermore, small percentages of cells in shapes other than biconcave disk will exist in any sample. Finally, it has been suggested that 5-NS-labeled erythrocytes undergo a velocity-dependent shape deformation under conditions similar to those employed in this work (Noji et al., 1981). Given these considerations, the assumption of two populations of erythrocytes, one perfectly aligned biconcave disks (with a single shape) and the second isotropic, is a considerable oversimplification of the actual situation.

In an effort to assess the influence of the simplified nature of this model on the values of α_1 and β_1 obtained, a second approach was employed. Using the fatty acid spin-label 5-NS, a model-independent membrane normal orientation distribution was determined, assuming that the nitroxide *z*-axis of 5-NS adopted a time-averaged orientation coincident with the membrane normal at all positions on the cell surface. This assumption appears to be well-justified on the basis of theoretical considerations (McConnell & McFarland, 1970) and numerous experimental studies conducted with this probe incorporated into oriented biological and model membranes over the past 25 years (Hubbell & McConnell, 1969). Simultaneous analysis of the linear EPR spectra (Figure 5) of 5-NS-labeled erythrocytes, oriented by flow through an EPR flat cell, gave a determination of the membrane normal orientation distribution, $N(\beta_2,\gamma_2)$, in terms of a set of linear coefficients of eq 23.

This membrane normal orientation distribution was then used to reanalyze the linear EPR spectra of SL-H_2DADS-maleimide-labeled band 3 in intact erythrocytes oriented by flow through an EPR flat cell as shown in Figure 6. The excellent agreement between the results obtained using this model-free approach ($\alpha_1 = 63°$ and $\beta_1 = 37°$) and those obtained using the model of Bitbol and Leterrier (1982) ($\alpha_1 = 58°$ and $\beta_1 = 36°$) demonstrates that the assumptions made in either approach do not have a strong influence on the numerical values of α_1 and β_1 obtained. It is interesting to note that the membrane normal distribution obtained from the lipid 5-NS probe appears to give a reasonable representation of the membrane normal distribution for band 3. This result would appear to rule out the possibility of large, flow-induced aggregates of protein or lipid.

The determination of the orientation of the nitroxide moiety of SL-H_2DADS-maleimide relative to the membrane normal axis in this study has important implications for previous studies by Hustedt and Beth (1995) which defined the orientation of the nitroxide moiety relative to the rotational diffusion axis, $\alpha = 66°$ and $\beta = 34°$ (Figure 1B). Collectively, these results indicate that the uniaxial diffusion axis and the membrane normal axis are coincident as predicted for the rotational diffusion of an intrinsic membrane protein (Saffman & Delbrück, 1975). This conclusion is important in establishing the reliability of SL-H_2DADS-maleimide as a probe of the global rotational dynamics of band 3 and the validity of the uniaxial rotational diffusion as a model for the observed dynamics. Any internal dynamic process of band 3 or of the spin-label relative to band 3, occurring on the micro- to millisecond time scale, would clearly interfere with the proper characterization of the global rotational dynamics and could in fact dominate the observed ST-EPR spectra. It is unlikely, from a purely probabilistic point of view, that such a process would happen to mimic a rotation about the membrane normal axis.

Uniqueness of the Determined Nitroxide Orientation. The possibility of multiple orientations of the nitroxide moiety relative to band 3 and, hence, to the membrane normal axis must be considered. It should be emphasized that work of Scothorn et al. described in the preceding paper has indicated that SL-H_2DADS-maleimide reacts with high specificity at the stilbenedisulfonate binding site of band 3, that approximately 1 mol of spin-label reacts per mole of band 3 monomer, that the reaction stoichiometrically inhibits anion exchange by band 3, and that the reaction is specific for a single proteolytic peptide of band 3. It has also been shown that SL-H_2DADS-maleimide and another anionic affinity probe for band 3, eosin-5-maleimide, label band 3 in a mutually exclusive manner. Although both probes label the same 17K proteolytic fragment, eosin-5-maleimide reacts exclusively with Lys-430 (Cobb & Beth, 1990) while SL-H_2DADS-maleimide reacts with either Lys-539 or Lys-542 (Scothorn et al., 1996). These results, together with information obtained on a number of other stilbenedisulfonate derivatives, strongly support a model where SL-H_2DADS-maleimide covalently reacts with high specificity at a single site on band 3 and that the probe is tightly held by some combination of the covalent coupling of the maleimide moiety, noncovalent interactions between the sulfonate groups and the basic amino acids of the stilbenedisulfonate binding site, and hydrogen bonding of the nitroxide moiety.

Tight binding of SL-H_2DADS-maleimide at a single site on band 3 is a necessary, but not sufficient, condition for the nitroxide adopting a single orientation or, more realistically, a narrow distribution of orientations about a single maximum. It could be argued that, using the model of Bitbol and Leterrier (1982), a broadly distributed population of nitroxide orientations was obscured in the analysis by the inclusion of a population of isotropically oriented, or spherical, erythrocytes which was necessary to fit the

experimental data (Figure 3). However, this argument is not as valid for the model-free analysis where an experimentally determined membrane normal orientation distribution obtained from the analysis of the linear EPR spectra of flow-oriented, 5-NS-labeled erythrocytes was used to analyze the data from SL-H_2DADS-maleimide bound to band 3 in intact erythrocytes (Figure 6). While a substantial population of nitroxides whose orientation with respect to the membrane normal is not within a narrow distribution about $\alpha_1 = 61°$ and $\beta_1 = 37°$ cannot be excluded solely on the basis of the results presented here, the absence of any significant systematic deviation of the fits from the data in Figure 6 strongly argues against such a possibility.

Implications of the Orientation Information Obtained in this Work on the Quaternary Structure of Band 3. Staros and Kakkad (1983) obtained data using two membrane impermeant cross-linking reagents which supported a model for band 3 in intact erythrocytes in which two subunits form a dimeric unit with a 2-fold axis of symmetry perpendicular to the plane of the membrane. More recently, Reithmeier and co-workers (Wang et al., 1993, 1994) have obtained two-dimensional crystals of the transmembrane domain of band 3 reconstituted in lipid bilayers which are suitable for image reconstruction of electron microscopy data. This latter study lends support to the hypothesis that two monomers of band 3 form a stable dimer having an extensive monomer−monomer interface and a 2-fold axis of symmetry. While several studies have provided evidence of higher oligomeric structures for band 3 (Jennings, 1984; Casey & Reithmeier, 1991), it appears likely that the fundamental oligomeric species of band 3 is a stable, symmetric dimer. The existence of a 2-fold symmetry axis for the dimer which is coincident with the membrane normal axis would dictate that the stilbenedisulfonate sites on each monomer are also related by symmetry. The orientation information obtained for the nitroxide moiety of SL-H_2DADS-maleimide in this work is entirely consistent with this proposal (although a mirror plane relating the two nitroxides cannot be excluded).

ACKNOWLEDGMENT

We are grateful to Dr. J. Feix for providing the [^{15}N,$^{2}H_{12}$]-5-NS spin-label, to Scott M. Blackman, Dr. Charles E. Cobb, and Dr. Joseph M. Beechem for helpful discussions, and to Dr. B. H. Robinson for critiquing the manuscript.

REFERENCES

Anjaneyulu, P. S. R., Beth, A. H., Sweetman, B. J., Faulkner, L. A., & Staros, J. V. (1988) *Biochemistry 27*, 6844−6851.

Anjaneyulu, P. S. R., Beth, A. H., Cobb, C. E., Juliao, S. F., Sweetman, B. J., & Staros, J. V. (1989) *Biochemistry 28*, 6583−6590.

Austin, R. H., Chan, S. S., & Jovin, T. M. (1979) *Proc. Natl. Acad. Sci. U.S.A. 76*, 5650−5654.

Balasubramanian, K., & Dalton, L. R. (1979) *J. Magn. Reson. 33*, 245−260.

Beechem, J. M., Gratton, E., Ameloot, M., Knutson, J. R., & Brand, L. (1991) in *Topics in Fluorescence Spectroscopy, Volume 2: Principles* (Lakowicz, J. R., Ed.) pp 241−305, Plenum Press, New York.

Beth, A. H., & Robinson, B. H. (1989) in *Biological Magnetic Resonance, Volume 8, Spin Labeling Theory and Applications* (Berliner, L. J., & Reuben, J., Eds.) pp 179−249, Plenum Press, New York.

Beth, A. H., Balasubramanian, K., Robinson, B. H., Dalton, L. R., Venkataramu, S. D., & Park, J. H. (1983) *J. Phys. Chem. 87*, 359−367.

Beth, A. H., Conturo, T. E., Venkataramu, S. D., & Staros, J. V. (1986) *Biochemistry 25*, 3824−3832.

Bitbol, M., & Leterrier, F. (1982) *Biorheology 19*, 669−680.

Burghardt, T. P., & Thompson, N. L. (1985) *Biophys. J. 48*, 401−409.

Burghardt, T. P., & French, A. R. (1989) *Biophys. J. 56*, 525−534.

Casey, J. R., & Reithmeier, R. A. F. (1991) *J. Biol. Chem. 266*, 15726−15737.

Cherry, R. J. (1978) *Methods Enzymol. 54*, 47−61.

Cherry, R. J. (1981) *Biochem. Soc. Symp. 46*, 183−190.

Cherry, R. J., & Godfrey, R. E. (1981) *Biophys. J. 36*, 257−276.

Cherry, R. J., Bürkli, A., Busslinger, M., Schneider, G., & Parish, G. R. (1976) *Nature 263*, 389−393.

Cobb, C. E., & Beth, A. H. (1990) *Biochemistry 29*, 8283−8290.

Cobb, C. E., Juliao, S. F., Balasubramanian, K., Staros, J. V., & Beth, A. H. (1990) *Biochemistry 29*, 10799−10806.

Corbett, J. D., & Golan, D. E. (1993) *J. Clin. Ivest. 91*, 208−217.

Delmelle, M., Butler, K. W., & Smith, I. C. P. (1980) *Biochemistry 19*, 698−704.

Evans, E., & Fung, Y.-C. (1972) *Microvasc. Res. 4*, 335−347.

Fajer, P. G. (1994) *Biophys. J. 66*, 2039−2050.

Fajer, P., & Marsh, D. (1983) *J. Magn. Reson. 51*, 446−459.

Gaffney, B. J. (1979) *J. Phys. Chem. 83*, 3345−3349.

Garland, P. B., & Johnson, P. (1985) in *The Enzymes of Biological Membranes, Volume 2* (Martonosi, A. N., Ed.) 2nd ed., pp 421−439, Plenum Press, New York.

Hubbell, W. L., & McConnell, H. M. (1969) *Proc. Natl. Acad. Sci. U.S.A. 64*, 20−27.

Hustedt, E. J., & Beth, A. H. (1994) *Biophys. J. 66*, A41.

Hustedt, E. J., & Beth, A. H. (1995) *Biophys. J. 69*, 1409−1423.

Hustedt, E. J., Cobb, C. E., Beth, A. H., & Beechem, J. M. (1993) *Biophys. J. 64*, 614−621.

Hyde, J. S., & Dalton, L. R. (1972) *Chem. Phys. Lett. 16*, 568−572.

Jennings, M. L. (1984) *J. Membr. Biol. 80*, 105−117.

Johnson, M. E., Lee, L., & Fung, L. W.-M. (1982) *Biochemistry 21*, 4459−4467.

Jovin, T. M., & Vaz, W. L. (1989) *Methods Enzymol. 172*, 471−513.

Libertini, L. J., Waggoner, A. S., Jost, P. C., & Griffith, O. H. (1969) *Proc. Natl. Acad. Sci. U.S.A. 64*, 13−19.

Marsden, J. E., & Tromba, A. J. (1976) *Vector Calculus*, p 383, Freeman and Co., San Francisco.

Mayatoshi, E. D., & Jovin, T. M. (1991) *Biochemistry 30*, 3527−3538.

McConnell, H. M., & McFarland, B. G. (1970) *Q. Rev. Biophys. 3*, 91−136.

McPherson, R. A., Sawyer, W. H., & Tilley, L. (1992) *Biochemistry 31*, 512−518.

McPherson, R. A., Sawyer, W. H., & Tilley, L. (1993) *Biochemistry 32*, 6696−6702.

Mühlebach, T., & Cherry, R. J. (1982) *Biochemistry 21*, 4225−4228.

Mühlebach, T., & Cherry, R. J. (1985) *Biochemistry 24*, 975−983.

Nigg, E., & Cherry, R. J. (1979a) *Nature 277*, 493−494.

Nigg, E. A., & Cherry, R. J. (1979b) *Biochemistry 18*, 3457−3465.

Nigg, E. A., & Cherry, R. J. (1980) *Proc. Natl. Acad. Sci. U.S.A. 77*, 4702−4706.

Noji, S., Inoue, F., & Kon, H. (1981) *Blood Cells 7*, 401−411.

Okubo, K., Kang, D., Hamasaki, N., & Jennings, M. L. (1994) *J. Biol. Chem. 269*, 1918−1926.

Press, W. H., Flannery, B. P., Teukolsky, S. A., & Vetterling, W. T. (1986) *Numerical Recipes*, Cambridge University Press, New York.

Saffman, P. G., & Delbrück, M. (1975) *Proc. Natl. Acad. Sci. U.S.A. 72*, 3111−3113.

Sakaki, T., Tsuji, A., Chang, C.-H., & Ohnishi, S.-I. (1982) *Biochemistry 21*, 2366−2372.

Scothorn, D. J., Wojcicki, W. E., Hustedt, E. J., Beth, A. H., & Cobb, C. E. (1996) *Biochemistry 35*, 6931−6943.

Staros, J. V., & Kakkad, B. P. (1983) *J. Membr. Biol. 74*, 247−254.

Thomas, D. D. (1985) Saturation transfer EPR studies of microsecond rotational motions in biological membranes, in *The Enzymes of Biological Membranes, Volume 2* (Martonosi, A. N., Ed.) 2nd ed., pp 287−312, Plenum Press, New York.

Thomas, D. D. (1986) Rotational diffusion of membrane proteins, in *Techniques for the Analysis of Membrane Proteins* (Ragan, C. I., & Cherry, R. J., Eds.) pp 377−431, Chapman and Hall, London.

Thomas, D. D., & McConnell, H. M. (1974) *Chem. Phys. Lett. 25*, 470−475.

Thomas, D. D., Dalton, L. R., & Hyde, J. S. (1976) *J. Chem. Phys. 65*, 3006−3024.

Tilley, L., Nash, G. R., Jones, G. L., & Sawyer, W. H. (1991) *J. Membr. Biol. 121*, 59−66.

Tsuji, A., Kawasaki, K., Ohnishi, S.-I., Merkle, H., & Kusumi, A. (1988) *Biochemistry 27*, 7447−7452.

Wang, D. N., Kühlbrandt, W., Sarabia, V. E., & Reithmeier, R. A. F. (1993) *EMBO J. 12*, 2233−2239.

Wang, D. N., Sarabia, V. E., Reithmeier, R. A. F., & Kühlbrandt, W. (1994) *EMBO J. 14*, 3230−3235.

Willingham, G. L., & Gaffney, B. J. (1983) *Biochemistry 22*, 892−898.

Wojcicki, W. E., & Beth, A. H. (1993) *Biophys. J. 64*, A308.

BI9601518